Design and Synthesis of Mesoporous Polymer-Based Solid Acid Catalysts with Excellent Hydrophobicity and Extraordinary Catalytic Activity

ARTICLE *in* ACS CATALYSIS · MARCH 2012

Impact Factor: 9.31 · DOI: 10.1021/cs200613p

5 AUTHORS, INCLUDING:

Fujian Liu
Zhejiang University
36 PUBLICATIONS **620** CITATIONS
SEE PROFILE

Weiping Kong
Chinese Academy of Sciences
7 PUBLICATIONS **76** CITATIONS
SEE PROFILE

ACS Catalysis

Research Article

pubs.acs.org/acscatalysis

Design and Synthesis of Mesoporous Polymer-Based Solid Acid Catalysts with Excellent Hydrophobicity and Extraordinary Catalytic Activity

Fujian Liu,*[,†] Weiping Kong,[†] Chenze Qi,[†] Longfeng Zhu,[§] and Feng-Shou Xiao*[,‡]

[†]Institute of Applied Chemistry, Department of Chemistry, Shaoxing University, Shaoxing 312000, China

[‡]Department of Chemistry, Zhejiang University, Hangzhou 310028, China

[§]Department of Chemistry, Jilin University, Changchun 130012, China

Supporting Information

ABSTRACT: Novel excellent hydrophobic- mesoporous- polymer-based solid acid catalysts have been successfully synthesized by copolymerization of divinylbenzene (DVB) with sodium *p*-styrene sulfonate (H-PDVB-*x*-SO_3H's) under solvothermal conditions. N_2 isotherms and TEM images showed that H-PDVB-*x*-SO_3H's have high BET surface areas, large pore volumes, and abundant mesoporosity; CHNS element analysis and acid−base titration technology showed that H-PDVB-*x*-SO_3H's have adjustable sulfur contents (0.31−2.36 mmol/g) and acidic concentrations (0.26−1.86 mmol/g); TG curves showed that H-PDVB-*x*-SO_3H's exhibited much higher stability of the active site (372 °C) than that of the acidic resin of Amberlyst 15 (312 °C); contact angle and water adsorption tests showed that H-PDVB-*x*-SO_3H's exhibited excellent hydrophobic properties. Catalytic tests in esterification of acetic acid with cyclohexanol, esterification of acetic acid with 1-butanol, and condensation of benzaldehyde with ethylene glycol showed that H-PDVB-*x*-SO_3H's were more active than those of Amberlyst 15, SO_3H-functionalized ordered mesoporous silicas, and beta and USY zeolites, which were even comparable with that of homogeneous H_2SO_4. The superior hydrophobicity of solid acid catalysts would be favorable for achieving excellent catalytic performance because water usually acts as a byproduct in various acid-catalyzed reactions, which can easily poison the acid sites and result in opposite reactions. Synthesis of porous solid acid catalysts with good hydrophobicity would be very important for their applications.

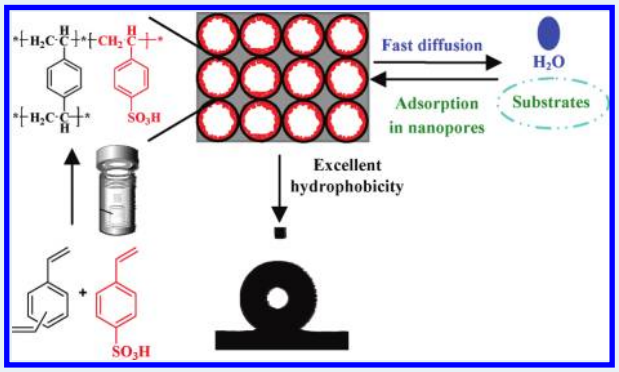

KEYWORDS: *mesoporous polymers, hydrophobicity, solid acid catalysts, copolymerization, acid-catalyzed liquid reactions*

INTRODUCTION

Solid acid catalysts have received much attention because of their potential applications for replacing mineral liquid acids in industry,[1−6] which exhibit the advantages of easy separation of the catalyst from the liquid reaction medium, reductive corrosion, good recyclability, green chemical processes, and enhanced product selectivity.[1−18]

Typically, solid acids such as zeolites[1,3,7−12] have been widely used in industry because of their high BET surface areas, adjustable frameworks, and shape-selectivity catalysis;[1,3] however, the small micropores (<1 nm) usually resulted in lower catalyzed conversion for bulky substrates.[1,3] The successfully synthesis of ordered mesoporous materials such as MCM-41 and SBA-15 offers great opportunity to solve the limitation of micropores[1,19−21] due to their larger and adjustable mesopores (2−50 nm). Until now, one of the most successful examples for applications of mesoporous silicas on heterogeneous acid catalysts was by grafting SO_3H groups onto the surface of the mesopore walls,[21−28] which exhibits very good catalytic activities in a series of acid-catalyzed reactions for bulky substrates.[22−32] However, zeolites or mesoporous silicas are composed of silica or silica−aluminum composites, which have shown hydrophilic properties in nature due to the presence of hydrophilic terminal silanols. The hydrophilic frameworks largely influence their catalytic activities because water usually acts as a byproduct in many acid-catalyzed reactions, which easily coadsorbs near the acid centers, resulting in their partial deactivation due to competition with the reactant species.[33−35]

It has been challenging to synthesize solid acids with excellent hydrophobicity up to now. Compared with hydrophilic inorganic networks, carbon and polymer networks exhibit hydrophobic features, which result in a new kind of solid acids by modification of sulfonic groups.[17,36−40] However, to the best of our knowledge, after grafting sulfonic groups, the hydrophobicity of their frameworks were thoroughly changed. For example, hydrophobic mesoporous carbon or resin becomes

Received: November 26, 2011
Revised: January 28, 2012

   dx.doi.org/10.1021/cs200613p | ACS Catal. 2012, 2, 565−572

hydrophilic after introduction of sulfonic acid groups;[36,39] Very recently, Liu et al. successfully synthesized novel superhydrophobic porous solid bases with very good catalytic activities in transesterifications,[41] which offers an opportunity to synthesize porous heterogeneous acid catalysts with superior hydrophobicity.

We demonstrate here a successful preparation of sulfonic group-functionalized, stable mesoporous solid acids with excellent hydrophobicity by copolymerization of divinylbenzene (DVB) with sodium *p*-styrene sulfonate (H-PDVB-*x*-SO_3H's) under solvothermal conditions without using any surfactant templates. H-PDVB-*x*-SO_3H samples have high BET surface areas, large pore volumes, adjustable active site concentrations, and excellent hydrophobicity. Catalytic tests have shown that H-PDVB-*x*-SO_3H's exhibit extraordinary catalytic activities and recyclability in esterifications of acetic acid with cyclohexanol (EAC), esterification of acetic acid with 1-butanol (EAB), and condensation of benzaldehyde with ethylene glycol (CBE), as compared with those of Amberlyst 15, sulfonic groups functional mesoporous silicas (SBA-15-SO_3H), and zeolites (USY and beta), which were even comparable with that of sulfuric acid in some cases.

EXPERIMENTAL DETAILS

Chemicals and Regents. All reagents were of analytical grade and used as purchased without further purification. Sodium *p*-styrene sulfonate, nonionic block copolymer surfactant poly(ethyleneoxide)−poly(propyleneoxide)−poly(ethyleneoxide) block copolymer (P123, molecular weight of ∼5800), 3-mercaptopropyltrimethoxysilane (3-MPTMS), and Amberlyst 15 were purchased from Sigma-Aldrich Company, Ltd. (USA). DVB, initiator of azobisisobutyronitrile (AIBN), tetraethyl orthosilicate (TEOS), H_2O_2 (30 wt %), benzaldehyde, ethylene glycol, 1-butanol, acetic acid, cyclohexanol, sulfuric acid, tetrahydrofuran (THF), dodecane, and sulfuric acid were obtained from Tianjin Guangfu Chemical Reagent. The H-form of beta zeolite and ultrastable Y zeolite (USY) were supplied by Sinopec Catalyst Co.

Catalyst Preparation. *Preparation of Mesoporous H-PDVB-x-SO_3H's.* Excellent hydrophobic mesoporous H-PDVB-*x*-SO_3H's (where *x* stand for the molar ratio of sodium *p*-styrene sulfonate with DVB) were solvothermally synthesized from copolymerization of DVB with sodium *p*-styrene sulfonate from the starting system of DVB/sodium *p*-styrene sulfonate/AIBN/THF/H_2O at a molar ratio of 1/*x*/0.02/16.1/7.23. As a typical run for the synthesis of H-PDVB-0.2-SO_3H, 2.0 g of DVB was added into a solution containing 0.05 g of AIBN and 20 mL of THF, followed by addition of 2.0 mL of H_2O, then 0.64 g of sodium *p*-styrene sulfonate was introduced. After stirring at room temperature for 3 h, the mixture was solvothermally treated at 100 °C for 24 h. After evaporation of the solvents at room temperature, the H-PDVB-0.2-SO_3Na sample with monolithic morphology was obtained.

To get a H-PDVB-0.2-SO_3H sample, the H-PDVB-0.2-SO_3Na sample was further ion-exchanged using 1 M sulfuric acid. As a typical run, 0.5 g of H-PDVB-0.2-SO_3Na was dispersed into 50 mL of 1 M sulfuric acid. After stirring for 24 h at room temperature, the sample was washed with a large amount of water until the filtrate was neutral. After drying at 80 °C for 12 h, H-PDVB-0.2-SO_3H was obtained.

For comparison, SBA-15-SO_3H with a molar ratio of S/Si at 0.1 and PDVB-SO_3H were synthesized according to the literature.[23,35] As a typical run for the synthesis of SBA-15-SO_3H, 4.0 g of P123 was dissolved in 125 g of 1.9 M HCl. After heating to 40 °C, 7.2 mL of TEOS was added to the above solution. After stirring for 40 min at 40 °C, 0.77 mL of 3-MPTMS and 1.25 g of (30 wt %) H_2O_2 was quickly added, and the solution was stirred for 20 h at 40 °C. Then the mixture was transferred into an autoclave and treated at 100 °C for 24 h. The removal of the P123 template was carried out by extraction of a mixture of ethanol and sulfuric acid, followed by washing with a large amount of water and drying at 60 °C.[23] As a typical run for synthesis of PDVB-SO_3H, 0.75 g of PDVB was outgassed at 100 °C in a three-necked round flask for 3 h. Then 50 mL of CH_2Cl_2 containing chlorosulfonic acid (10 mL) was added into the flask at 0 °C, and the solution was stirred for 12 h under a nitrogen atmosphere. Finally, a yellow PDVB-SO_3H sample with powder morphology was obtained.[35]

Characterization. Nitrogen isotherms were measured using a Micromeritics ASAP 2020 M system. The samples were outgassed for 10 h at 150 °C before the measurements, and the pore-size distribution for mesopores was calculated using the Barrett−Joyner−Halenda (BJH) model. FTIR spectra were recorded by using a Bruker 66 V FTIR spectrometer. Thermogravimetric analyses (TG) were performed on a Perkin-Elmer TGA7 in flowing air a the heating rate of 20 °C/min. The acid-exchange capacities of the catalysts were determined by acid−base titration with standard NaOH solution. XPS spectra were performed on a Thermo ESCALAB 250 with Al Kα radiation, and binding energies were calibrated using the C1s peak at 284.9 eV. Contact angles were tested on a DSA10MK2G140 (Kruss Company, Germany) at 25 °C. Water adsorption was carried out using a sorption analyzer (MB-300G) at 25 °C with different humidities. Before measurement, a certain amount (∼50 mg) of the samples was treated for 10 h at 150 °C under vacuum, then the sample was exposed to water vapor at different humidities, which could be adjusted by controlling the vapor pressure. CHNS elemental analyses were performed on a Perkin-Elmer series II CHNS analyzer 2400. TEM images were performed on a FEI Tecnai G2 F20 s-twin D573 transmission electron microscope working at 200 kV.

Catalytic Tests. Esterifications of acetic acid with cyclohexanol were performed by mixing and stirring 0.2 g of catalyst and 11.5 mL (0.11 mol) of cyclohexanol in a three-necked round flask equipped with a condenser and a magnetic stirrer. After heating the mixture to 100 °C using an oil bath, 17.5 mL (0.305 mol) of acetic acid was rapidly added, followed by the reaction for 1 h. In this reaction, the molar ratio of acetic acid/cyclohexanol was 2.6. The product was cyclohexyl acetate with selectivity higher than 99.5%.

Esterification of acetic acid with 1-butanol was performed by mixing 0.01 g of catalyst, 50 mmol of acetic acid, and 50 mmol of *n*-butanol in a glass flask equipped with a condenser and a magnetic stirrer. After the temperature was increased to 90 °C, the reaction was allowed to continue for 4 h. In this reaction, the molar ratio of acetic acid/*n*-butanol was 1.5. The product was 1-butyl acetate with selectivity higher than 99.5%.

Condensation of benzaldehyde with ethylene glycol was performed by mixing and stirring of 0.01 g of catalyst and 15 mmol of benzaldehyde in a three-necked round flask equipped with a condenser and a magnetic stirrer. After heating the mixture to 90 °C using an oil bath, 15 mmol of ethylene glycol was rapidly added, followed by allowing the reaction to continue for 1 h. In this reaction, the molar ratio of benzaldehyde/ethylene glycol was 1.0. The product was 2-phenyl-1,3-dioxolane with a selectivity higher than 99.5%.

All the reactions were analyzed by gas chromatography (Agilent 7890) with a flame ionization detector (FID), and

dx.doi.org/10.1021/cs200613p | ACS Catal. 2012, 2, 565−572

dodecane was used as an internal standard. The column was a HP-INNOWax capillary column (30 m). The initial temperature was 100 °C, the temperature ramp rate was 20 °C/min, and the final temperature was 280 °C. The temperature of the FID detector was 300 °C.

RESULTS AND DISCUSSION

Figure 1 shows N_2 isotherms and the corresponding pore size distribution of H-PDVB-*x*-SO_3H's synthesized with different

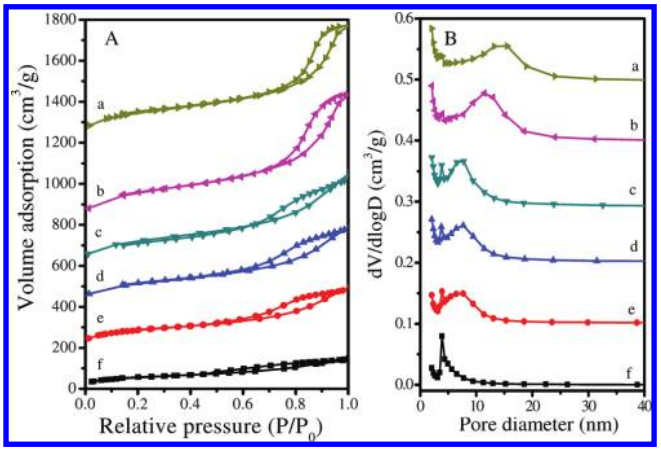

Figure 1. (A) N_2 adsorption−desorption isotherms and (B) the corresponding pore size distribution of (a) H-PDVB-0.05-SO_3H, (b) H-PDVB-0.1-SO_3H, (c) H-PDVB-0.2-SO_3H, (d) H-PDVB-0.33-SO_3H, (e) H-PDVB-0.5-SO_3H, and (f) H-PDVB-1.0-SO_3H. The isotherms for a−e were offset by 1200, 800, 600, 400, and 200 cm^3/g along with the vertical axis for clarity, and the pore size distributions for a−e were offset by 0.5, 0.4, 0.3, 0.2, and 0.1 cm^3/g, respectively, along with vertical axis for clarity.

molar ratios of sodium *p*-styrene sulfonate to DVB. Clearly, all the samples showed typical type-IV isotherms, giving a steep increase at a relative pressure of $0.6 < P/P_0 < 0.9$, indicating the presence of mesoporosity.[42] It is worth noting that with an increase in the content of sodium *p*-styrene sulfonate, the BET surface areas and pore volumes tend to decrease. For example, when the molar ratio of sodium *p*-styrene sulfonate to DVB was 0.1, it resulted in H-PDVB-0.1-SO_3H, which showed the BET surface area and pore volume of 535 m^2/g and 0.99 cm^3/g, respectively (Table 1, run 2), higher than that of H-PDVB-1.5-SO_3H (143 m^2/g and 0.21 cm^3/g, Table 1, run 8), thus confirming that the higher content of sodium *p*-styrene sulfonate may not be helpful for the formation of the sample with abundant mesoporosity. Obviously, the BET surface areas of H-PDVB-*x*-SO_3H samples were much higher than that of Amberlyst 15 (45 m^2/g, Table 1, run 10) but lower than that of SBA-15-SO_3H (820 m^2/g, Table S1 of the Supporting Information, run 11). More interestingly, H-PDVB-*x*-SO_3H's have stable mesoporosity. For example, compared with fresh H-PDVB-0.33-SO_3H (BET surface area of 377 m^2/g and pore volume of 0.46 cm^3/g), even after five catalytic recycles, there was no obvious decrease in the sample BET surface area (364 m^2/g) and large volume (0.45 cm^3/g, Table 1 Run 5). These results demonstrate that H-PDVB-*x*-SO_3H's could be used as stable heterogeneous acid catalysts for recyclability.

It is noteworthy that the solvothermal conditions play a key role in the formation of abundant mesoporosity in the samples. In this work, the solvothermal route provides a sealed media in which most of the solvents remained in the liquid phase at relatively high temperatures (100 °C) and high pressure. When DVB and styrene-*p*-sulfonate monomers started to polymerize under these conditions, a loose but highly cross-linked network was gradually formed in the solvent (THF and water), which is considered both solvent and the unique "template". After the removal of large amount of the solvents as the guest, H-PDVB-*x*-SO_3H samples with open disordered and uniform porosity (in the range of mesoporosity, pore diameter around 3−20 nm) were finally obtained. A similar phenomenon has also been discussed in the literature.[41,43]

Table 1 presents the sulfur content and acid concentration of H-PDVB-*x*-SO_3H samples, indicating adjustable contents of acidic concentration between 0.26 and 1.86 mmol/g (Table 1, Run 1−8), much lower than that of PDVB-SO_3H (sulfonic group functional PDVB by sulfonation using chlorosulfonic acid, 4.0 mmol/g, Table 1, run 9) or Amberlyst 15 (4.7 mmol/g, Table 1, run 10). Moreover, the recycled H-PDVB-0.33-SO_3H showed nearly no obvious decreases in both acidic concentration and sulfur content as compared with those of the fresh one (Table 1, run 5).

Figure 2 showed the TEM images of H-PDVB-0.2-SO_3H and H-PDVB-0.33-SO_3H. Both showed abundant wormhole-like mesopores with a broad pore size distribution ranging from 3 to

Table 1. The Textural and Acidic Parameters of Various Solid Acid Catalysts

run	samples	S content (mmol/g)[a]	acid sites (mmol/g)[b]	S_{BET} (m^2/g)	V_p (cm^3/g)	D_p (nm)[c]
1	H-PDVB-0.05-SO_3H	0.31	0.26	472	0.87	14.3
2	H-PDVB-0.1-SO_3H	0.60	0.48	535	0.99	11.7
3	H-PDVB-0.2-SO_3H	0.88	0.76	433	0.50	7.2
4	H-PDVB-0.33-SO_3H	1.31	1.02	377	0.46	7.3
5	H-PDVB-0.33-SO_3H[d]	1.28	1.01	364	0.45	7.1
6	H-PDVB-0.5-SO_3H	1.78	1.24	316	0.36	7.0
7	H-PDVB-1.0-SO_3H	1.96	1.53	194	0.18	3.9
8	H-PDVB-1.5-SO_3H	2.36	1.86	143	0.21	7.6
9	PDVB-SO_3H	3.64	4.00	380	0.90	23.5
10	Amberlyst 15	4.30	4.70	45	0.31	40
11	SBA-15-SO_3H	1.36	1.26	820	1.40	7.3
12	H-beta[e]		1.21	550	0.20	0.67
13	H-USY[f]		2.06	623	0.26	14.7
14	H_2SO_4	10.2	20.4			

[a]Measured by elemental analysis. [b]Measured by acid−base titration. [c]Pore size distribution estimated from BJH model. [d]The sample recycled five times in esterification of acetic acid with cyclohexanol. [e]Si/Al ratio at 12.5. [f]Si/Al ratio at 7.5.

dx.doi.org/10.1021/cs200613p | ACS Catal. 2012, 2, 565−572

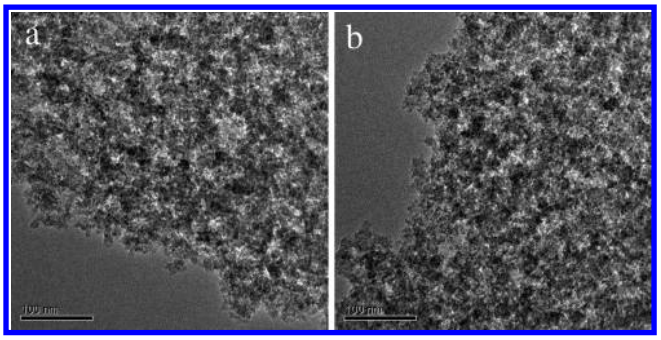

Figure 2. TEM images of (a) H-PDVB-0.2-SO_3H and (b) H-PDVB-0.33-SO_3H.

20 nm, in good agreement with the data from N_2 adsorption isotherms.

Figure 3 shows the hydrophobicity tests over various samples. When a water droplet contact H-PDVB-0.05-SO_3H, it yielded a contact angle up to 152° (Figure 3a), which indicates its superhydrophobicity. In addition, for the samples with different molar ratios of sodium *p*-styrene sulfonate with DVB (H-PDVB-*x*-SO_3H, x = 0.1−1.5), the contacted angles were 148−118° (Figure 3B−G), which confirms their excellent hydrophobicity. In contrast, PDVB-SO_3H and Amberlyst 15 showed contact angles of 38° and 8°, respectively (Figure 2h and i), indicating their good hydrophilicity. To the best of our knowledge, few investigations on synthesis of solid acid catalysts with excellent hydrophobicity exist.

Figure S1 shows contacted angles of substrate droplets of cyclohexanol, 1-butanol, acetic acid, glycol, and benzaldehyde on the surface of H-PDVB-0.33-SO_3H, a range of 0−25°. These results demonstrate that H-PDVB-*x*-SO_3H's have good wettability for various organic compounds.

Figure 4 shows the water adsorption properties over H-PDVB-0.33-SO_3H, SBA-15-SO_3H, and Amberlyst 15 under different humidities. Interestingly, H-PDVB-0.33-SO_3H exhibited a much lower adsorption capacity for water as compared with that of SBA-15-SO_3H and Amberlyst 15. For example, when the relative humidity was 60%, H-PDVB-0.33-SO_3H showed an adsorption capacity for water only at 2.65 wt %. In contrast, SBA-15-SO_3H and Amberlyst 15 showed an adsorption capacity for water at 18.2 and 32 wt %. Even after increasing the relative humidity to 94%, the adsorption capacity of H-PDVB-0.33-SO_3H for water was increased to 5.8 wt %, much lower than that of SBA-15-SO_3H (54.8%) and Amberlyst 15 (50.6%),

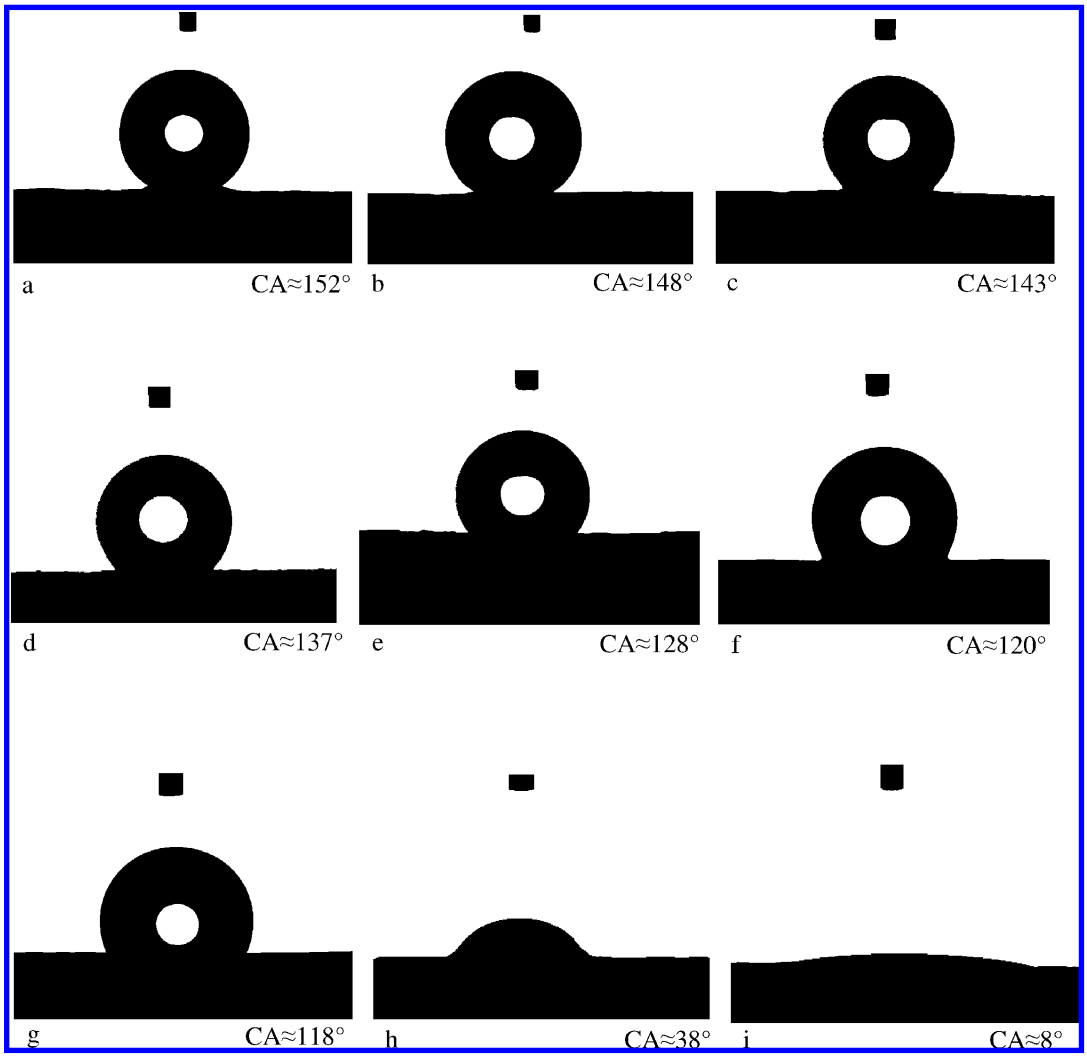

Figure 3. Contact angles of water droplets on the surface of (a) H-PDVB-0.05-SO_3H, (b) H-PDVB-0.1-SO_3H, (c) H-PDVB-0.2-SO_3H, (d) H-PDVB-0.33-SO_3H, (e) H-PDVB-0.5-SO_3H, (f) H-PDVB-1.0-SO_3H, (g) H-PDVB-1.5-SO_3H, (h) PDVB-SO_3H, and (i) Amberlyst 15 samples.

dx.doi.org/10.1021/cs200613p | *ACS Catal.* 2012, 2, 565−572

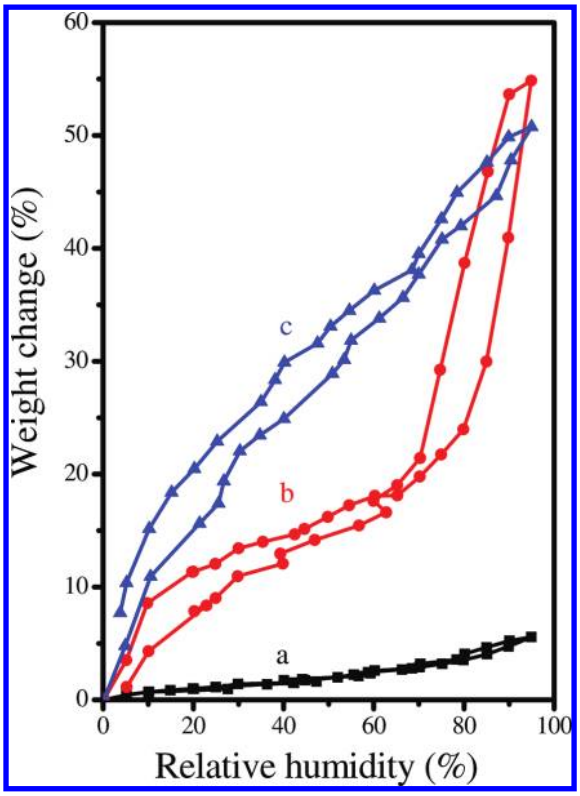

Figure 4. Water isotherms of (a) H-PDVB-0.33-SO_3H, (b) SBA-15-SO_3H, and (c) Amberlyst 15 under different humidities.

demonstrating the excellent hydrophobicity of H-PDVB-0.33-SO_3H, in good agreement with the contact angle tests.

Figure 5 shows FT-IR spectra of H-PDVB-*x*-SO_3H's samples at 1010, 1035, 1125, and 1174 cm^{-1}. Notably, the band at around

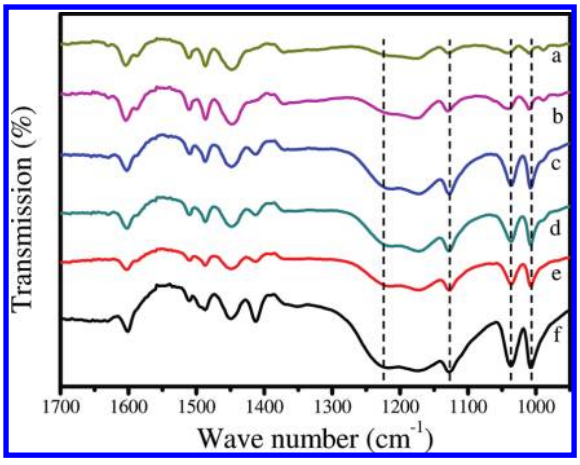

Figure 5. FT-IR spectra of (a) H-PDVB-0.05-SO_3H, (b) H-PDVB-0.1-SO_3H, (c) H-PDVB-0.2-SO_3H, (d) H-PDVB-0.33-SO_3H, (e) H-PDVB-0.5-SO_3H, and (f) H-PDVB-1.0-SO_3H samples.

1035 cm^{-1} is associated with the presence of a C−S bond on the benzene rings, and the bands at around 1010, 1125, and 1174 cm^{-1} are associated with the asymmetric and symmetric stretching signals of the O═S═O bonds of a sulfonic group.[35,36] These results indicate the successful introduction of sulfonic groups onto the network of mesoporous polymers through the copolymerization route.

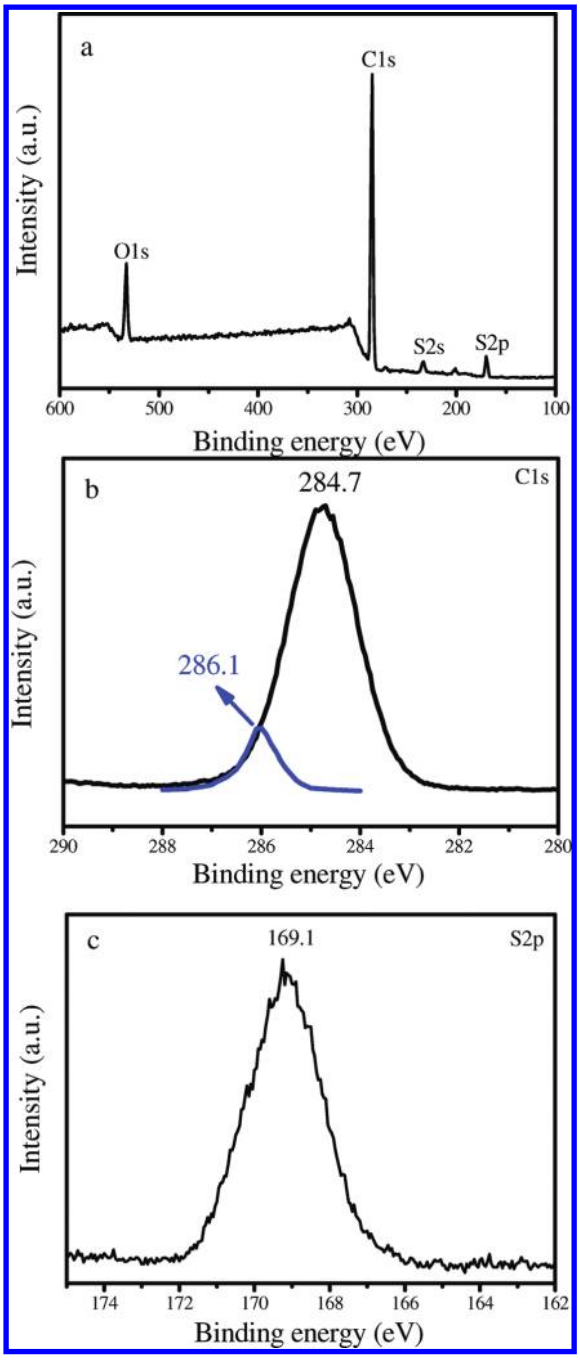

Figure 6. XPS measurements of (a) survey, (b) C 1s, and (c) S 2p spectra over the H-PDVB-0.33-SO_3H sample.

Figure 6 shows the XPS measurements of H-PDVB-0.33-SO_3H, which exhibits the obvious signals of C, S, and O elements. The S 2p and S 2s peaks at 169.1 and 233 eV (Figure 6A) are assigned to S−O and S═O bonds. The C 1s peaks around 284.8 and 286.1 eV (Figure 6B) are associated with C−C and C−S bonds,[44] confirming the sulfonic groups functionalized on the polymer network, in good agreement with results obtained from FT-IR spectrosocpy.

Figure 7 shows the TG curves of H-PDVB-0.33-SO_3H and Amberlyst 15. Both samples show a weight loss at 30−150, 240−465, and 470−590 °C, which are assigned to desorption of water, decomposition of sulfonic groups, and destruction of

dx.doi.org/10.1021/cs200613p | ACS Catal. 2012, 2, 565−572

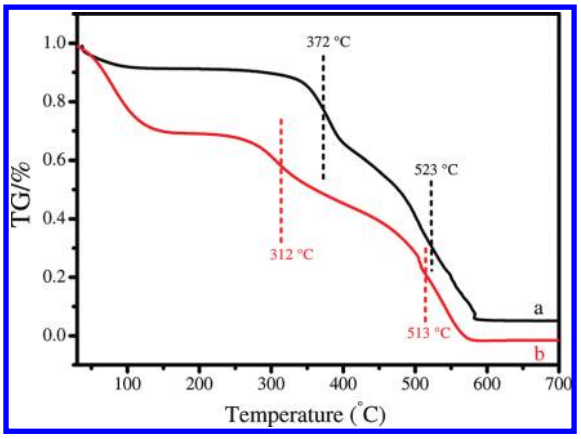

Figure 7. TG curves of (a) H-PDVB-0.33-SO_3H and (b) Amberlyst 15.

the polymer network, respectively.[45−47] Interestingly, between 30 and 150 °C, H-PDVB-0.33-SO_3H showed a much lower weight loss as compared with that of Amberlyst 15, indicating the lower adsorption content for the water in the air, which may be due to its excellent hydrophobicity. Moreover, with increasing temperature, H-PDVB-0.33-SO_3H exhibited the decomposition temperature of sulfonic groups and network at 372 and 523 °C, respectively, which were much higher than that of Amberlyst 15 (312 and 513 °C). These results demonstrate that H-PDVB-0.33-SO_3H has a much better thermal stability than that of Amberlyst 15, which is very favorable for catalyst recycling.

Table 2 presents catalytic data in the reactions of EAC, EAB, and CBE over various catalysts. Clearly, H-PDVB-*x*-SO_3H samples showed much higher catalytic activities in both esterifications and condensation than did the solid acids of Amberlyst 15, SBA-15-SO_3H, and beta and USY zeolites. In some cases, the activities of H-PDVB-*x*-SO_3H samples were even comparable with those of H_2SO_4. For example, in the reaction of EAC, H-PDVB-0.33-SO_3H showed conversion of cyclohexanol at 78.1%, giving TOF of 421 h^{-1} (Table 2, run 4), which was much higher than those of PDVB-SO_3H (conversion of 55.2% and TOF of 76 h^{-1}, Table 2, run 10), Amberlyst 15 with beads morphology (conversion of 42.7% and TOF of 50 h^{-1}, Table 2, run 11). Similar trends could also be found in the reaction of EAB.

Notably, except for esterifications, H-PDVB-*x*-SO_3H's also showed very good catalytic activities (76.7−91.4%, Table 2, runs 1−9) in the reaction of CBE. For example, H-PDVB-0.33-SO_3H showed a conversion of benzaldehyde at 89.3%, giving TOF values of 1313 h^{-1} (Table 2, run 4), which is much higher than those of PDVB-SO_3H (conversion of 77.6% and TOF of 291 h^{-1}, Table 2, run 10) and Amberlyst 15 (conversion of 70.8% and TOF of 226 h^{-1}, Table 2, run 11). Particularly, the TOF of H-PDVB-0.33-SO_3H (1313 h^{-1}) was even higher than that of H_2SO_4 (1218 h^{-1}), which is reasonably related to its excellent hydrophobicity (Figure 3) and good wettability for substrates (Figure S1 of the Supporting Information).

Table 2. Catalytic Data in Esterification of Acetic Acid with Cyclohexanol, Esterification of Acetic Acid with 1-Butanol, and Condensation of Benzaldehyde with Ethylene Glycol

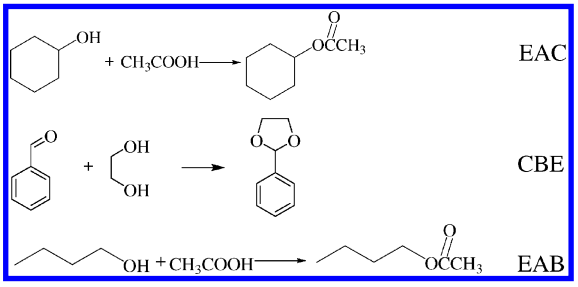

		EAC[a]		EAB[b]		CBE[c]	
run	samples	conv (%)	TOF[d] (h^{-1})	conv (%)	TOF[d] (h^{-1})	conv (%)	TOF[d] (h^{-1})
1	H-PDVB-0.05-SO_3H	55.1	1166	69.8	3356	76.8	4431
2	H-PDVB-0.1-SO_3H	69.2	793	87.2	2271	82.7	2584
3	H-PDVB-0.2-SO_3H	77.2	559	87.9	1446	91.4	1804
4	H-PDVB-0.33-SO_3H	78.1	421	89.9	1102	89.3	1313
5	H-PDVB-0.33-SO_3H[e]	76.4	412	84.5	1078	89.6	1318
6	H-PDVB-0.33-SO_3H[f]	74.5	402	82.3	1051	84.7	1246
7	H-PDVB-0.5-SO_3H	75.3	334	82.0	827	85.3	1032
8	H-PDVB-1.0-SO_3H	67.2	242	85.6	699	83.0	814
9	H-PDVB-1.5-SO_3H	58.1	172	82.7	556	83.8	676
10	PDVB-SO_3H	55.2	76	79.1	247	77.6	291
11	Amberlyst 15	42.7	50	60.8	162	70.8	226
12	Amberlyst 15[g]	49.8	58	68.2	181	74.6	238
13	SBA-15-SO_3H	30.3	132	46.9	465	55.2	657
14	H-beta	19.8	90	38.7	400	40.1	497
15	H-USY	24.7	66	40.2	244	44.9	327
16	H_2SO_4[h]	80.3	433	88.2	1081	82.8	1218

[a]The activities in EAC were evaluated by cyclohexanol conversion. [b]The activities in EAB were evaluated by butanol conversion. [c]The activities in CBE were evaluated by benzaldehyde conversion. [d]Turnover frequency (TOF, h^{-1}). [e]Recycled three times. [f]Recycles for five times. [g]Powder Amberlyst 15 catalyst. [h]The same amount of acidic sites as that of H-PDVB-0.33-SO_3H.

dx.doi.org/10.1021/cs200613p | ACS Catal. 2012, 2, 565−572

It is also observed that PDVB-SO_3H and H-PDVB-*x*-SO_3H samples have very similar polymer networks and sulfonic groups, but they have quite different catalytic activities. The PDVB-SO_3H sample was synthesized from the sulfonation of mesoporous PDVB materials,[35] and H-PDVB-*x*-SO_3H samples resulted from copolymerization of DVB with *p*-styrene sulfonate under solvothermal conditions. The major difference between PDVB-SO_3H and H-PDVB-*x*-SO_3H's is their distinguishing contact angles of water droplets on the sample surface (Figure 3). Therefore, it is reasonably suggested that the sample hydrophobicity and wettability for various organic substrates (Figure S1) play important roles in the contribution of catalytic activities.

To compare various catalysts, we also tested the catalytic kinetics of H-PDVB-0.2-SO_3H, H-PDVB-0.33-SO_3H, PDVB-SO_3H, Amberlyst 15, and homogeneous H_2SO_4 (Figure 8).

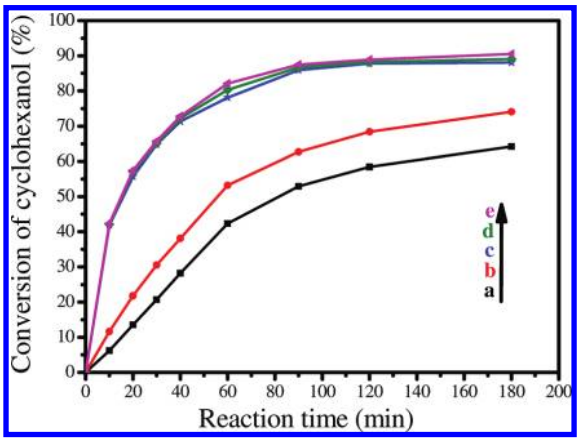

Figure 8. Catalytic kinetics of (a) Amberlyst 15, (b) PDVB-SO_3H, (c) H-PDVB-0.33-SO_3H, (d) H_2SO_4, and (e) H-PDVB-0.2-SO_3H. The acidic sites of c, d, and e are the same.

Clearly, H-PDVB-0.2-SO_3H and H-PDVB-0.33-SO_3H showed much higher catalytic rates than PDVB-SO_3H and Amberlyst 15, which were almost similar to that of H_2SO_4. For example, H-PDVB-0.33-SO_3H showed the conversion of cyclohexanol at 41.9% when the reaction ran for 10 min, but PDVB-SO_3H and Amberlyst 15 exhibited conversion of 11.6 and 6.2% under the same conditions. This activity of H-PDVB-0.33-SO_3H is comparable with that of H_2SO_4 (conversion of 42.5%).

Moreover, H-PDVB-*x*-SO_3H's have very good recyclability. For example, in the EAC reaction, even after being recycled three and five times, H-PDVB-0.33-SO_3H still exhibits very high catalytic activities of 76.4% (Table 2, run 5) and 74.5% (Table 2, run 6), respectively. In addition, the catalytic kinetics of recycled samples in the EAC reaction confirmed the extraordinary recyclability of the H-PDVB-0.33-SO_3H sample (Figure S2). Similarly, the tests of EAB and the reactions also demonstrate that H-PDVB-0.33-SO_3H has a very good recyclability.

CONCLUSION

Novel excellently hydrophobic mesoporous solid acids of H-PDVB-*x*-SO_3H have been successfully prepared by copolymerization of DVB with sodium *p*-styrene sulfonate under solvothermal conditions. H-PDVB-*x*-SO_3H's have high BET surface areas, adjustable acidic concentrations, and good thermal stability. More interestingly, compared with various solid acids, H-PDVB-*x*-SO_3H's have extraordinary catalytic activities in esterifications and condensation, better than that of SBA-15-SO_3H, Amberlyst 15, and zeolites, which were comparable with that of H_2SO_4. More importantly, H-PDVB-*x*-SO_3H's have very good recyclability. The superior catalytic performance of H-PDVB-*x*-SO_3H's is attributed to the unique feature of excellent hydrophobicity and good wettability for the substrates.

ASSOCIATED CONTENT

Supporting Information

Additional information as noted in text. This material is available free of charge via the Internet at http://pubs.acs.org.

AUTHOR INFORMATION

Corresponding Author

*Phone: +86-575-88341832. Fax: +86-575-88341832. E-mail: liufujian1982@yahoo.cn.

Notes

The authors declare no competing financial interest.

REFERENCES

(1) Corma, A. *Chem. Rev.* **1997**, *97*, 2373−2419.
(2) Corma, A. *Chem. Rev.* **1995**, *95*, 559−614.
(3) Davis, M. E. *Nature* **2002**, *417*, 813−821.
(4) Jones, C. W.; Tsuji, K.; Davis, M. E. *Nature* **1998**, *393*, 52−54.
(5) Corma, A.; García, H. *Chem. Rev.* **2003**, *103*, 4307−4366.
(6) Wong, W.-L.; Ho, K.-P.; Lee, L. Y. S.; Lam, K.-M.; Zhou, Z.-Y.; Chan, T. H.; Wong, K.-Y. *ACS Catal.* **2011**, *1*, 116−119.
(7) Xiao, F.-S.; Wang, L. F.; Yin, C. Y.; Lin, K. F.; Di, Y.; Li, J.; Xu, R.; Su, D. S.; Schlögl, R.; Yokoi, T.; Tatsumi, T. *Angew. Chem., Int. Ed.* **2006**, *45*, 3090−3093.
(8) Choi, M.; Na, K.; Kim, J.; Sakamoto, Y.; Terasaki, O.; Ryoo, R. *Nature* **2009**, *461*, 246−249.
(9) Fan, W.; Snyder, M. A.; Kumar, S.; Lee, P. S.; Yoo, W. C.; McCormick, A. V.; Penn, R. L.; Stein, A.; Tsapatsis, M. *Nat. Mater.* **2008**, *7*, 984−991.
(10) Tao, Y. S.; Kanoh, H.; Abrams, L.; Kaneko, K. *Chem. Rev.* **2006**, *106*, 896−910.
(11) Xu, R. R.; Pang, W. Q.; Yu, J. H.; Huo, Q. S.; Chen, J. S. *Chemistry of Zeolite and Related Porous Materials*; Wiley-VCH: Singapore, 2007.
(12) Nikolla, E.; Román-Leshkov, Y.; Moliner, M.; Davis, M. E. *ACS Catal.* **2011**, *1*, 408−410.
(13) López, D. E.; Goodwin, J. G. Jr.; Bruce, D. A. *J. Catal.* **2007**, *245*, 381−391.
(14) Barbaro, P.; Liguori, F. *Chem. Rev.* **2009**, *109*, 515−529.
(15) Mizuno, N.; Misono, M. *Chem. Rev.* **1998**, *98*, 199−218.
(16) Clark, J. H. *Acc. Chem. Res.* **2002**, *35*, 791−797.
(17) Huber, G. W.; Chheda, J. N.; Barrett, C. J.; Dumesic, J. A. *Science* **2005**, *308*, 1446−1450.
(18) Harmer, M. A.; Sun, Q. *Appl. Catal., A* **2001**, *221*, 45−62.
(19) Kresge, C. T.; Leonowicz, M. E.; Roth, W. J.; Vartuli, J. C.; Beck, J. S. *Nature* **1992**, *359*, 710−712.
(20) Zhao, D. Y.; Feng, J.; Huo, Q.; Melosh, N.; Fredrickson, G. H.; Chmelka, B. F.; Stucky, G. D. *Science* **1998**, *279*, 548−552.
(21) De Vos, D. E.; Dams, M.; Sels, B. F.; Jacobs, P. A. *Chem. Rev.* **2002**, *102*, 3615−3640.
(22) Melero, J. A.; Van Grieken, R.; Morales, G. *Chem. Rev.* **2006**, *106*, 3790−3812.
(23) Margolese, D.; Melero, J. A.; Christiansen, S. C.; Chmelka, B. F.; Stucky, G. D. *Chem. Mater.* **2000**, *12*, 2448−2459.
(24) Díaz, I.; Márquez-Alvarez, C.; Mohino, F.; Pérez-Pariente, J.; Sastre, E. *J. Catal.* **2000**, *193*, 283−294.
(25) Yang, Q. H.; Liu, J.; Zhang, L.; Li, C. *J. Mater. Chem.* **2009**, *19*, 1945−1955.
(26) Stein, A.; Melde, B. J.; Schroden, R. C. *Adv. Mater.* **2000**, *12*, 1403−1419.

(27) Li, C. M.; Yang, J.; Wang, P. Y.; Liu, J.; Yang, Q. H. *Microporous Mesoporous Mater.* **2009**, *123*, 228−233.
(28) Martín, A.; Morales, G.; Martínez, F.; van Grieken, R.; Gao, L.; Kruk, M. *J. Mater. Chem.* **2010**, *20*, 8026−8035.
(29) Yang, Q. H.; Liu, J.; Yang, J.; Kapoor, M. P.; Inagaki, S.; Li, C. *J. Catal.* **2004**, *228*, 265−272.
(30) Bossaert, W. D.; De Vos, D. E.; Van Rhijn, W. M.; Bullen, J.; Grobet, P. J.; Jacobs, P. A. *J. Catal.* **1999**, *182*, 156−164.
(31) Melero, J. A.; Stucky, G. D.; Griekena, R. V.; Morales, G. *J. Mater. Chem.* **2002**, *12*, 1664−1670.
(32) Wight, A. P.; Davis, M. E. *Chem. Rev.* **2002**, *102*, 3589−3614.
(33) Morales, G.; Athens, G.; Chmelka, B. F.; van Grieken, R.; Melero, J. A. *J. Catal.* **2008**, *254*, 205−217.
(34) Okuhara, T. *Chem. Rev.* **2002**, *102*, 3641−3666.
(35) Liu, F. J.; Meng, X. J.; Zhang, Y. L.; Ren, L. M.; Nawaz, F.; Xiao, F.-S. *J. Catal.* **2010**, *271*, 52−58.
(36) Xing, R.; Liu, N.; Liu, Y. M.; Wu, H. H.; Jiang, Y. W.; Chen, L.; He, M. Y.; Wu, P. *Adv. Funct. Mater.* **2007**, *17*, 2455−2461.
(37) Long, W.; Jones, C. W. *ACS Catal.* **2011**, *1*, 674−681.
(38) Hara, M.; Yoshida, T.; Takagaki, A.; Takata, T.; Kondo, J. N.; Hayashi, S.; Domen, K. *Angew. Chem., Int. Ed.* **2004**, *43*, 2955−2958.
(39) Wang, X. Q.; Liu, R.; Waje, M. M.; Chen, Z. W.; Yan, Y. S.; Bozhilov, K. N.; Feng, P. Y. *Chem. Mater.* **2007**, *19*, 2395−2397.
(40) Takagaki, A.; Takahashi, M.; Nishimura, S.; Ebitani, K. *ACS Catal.* **2011**, *1*, 1562−1565.
(41) Liu, F. J.; Li, W.; Sun, Q.; Zhu, L. F.; Meng, X. J.; Guo, Y. H.; Xiao, F.-S. *ChemSusChem* **2011**, *4*, 1059−1062.
(42) Zhao, D. Y.; Huo, Q. S.; Feng, J. L.; Chmelka, B. F; Stucky, G. D. *J. Am. Chem. Soc.* **1998**, *120*, 6024−6036.
(43) Zhang, Y. L.; Wei, S.; Liu, F. J.; Du, Y. C.; Liu, S.; Ji, Y. Y.; Yokoi, T.; Tatsumi, T.; Xiao, F.-S. *Nano. Today.* **2009**, *4*, 135−142.
(44) Koibeck, C.; Killian, M.; Maier, F.; Paape, N.; Wasserscheid, P.; Steinrück, H.-P. *Langmuir* **2008**, *24*, 9500−9507.
(45) Inczédy, J. *J. Therm. Anal.* **1978**, *13*, 257−261.
(46) Bother, N.; Descher, F.; Klein, J.; Widdecke, H. *Polymer* **1979**, *20*, 850−854.
(47) Widdecke, H. *Brit. Polym.* **1984**, *16*, 188−192.